Characterization of CNTs and CNTs/MnO_2 Composite for Supercapacitor Application

Aydın Toygan MUTLU

Directosr: Prof. Enric Bertran Serra and Dr.Roger Amade Rovira, Department of Applied Physics and Optics, Universitat de Barcelona, c/Martí i Franquès 1, 08028 Barcelona, Spain

***Abstract*- Manganese oxide (MnO_2) was deposited on multiwalled carbon nanotubes (MWCNTs) via electrochemical deposition technique. Morphological and structural characterizations were examined using Scanning Electron Microscopy (SEM), Transmission Electron Microscopy (TEM) and Raman Spectroscopy. Cyclic voltammetry and Galvanostatic charge-discharge measurements were performed to study the electrochemical properties. *0.2 M* Na_2SO_4 was used as an electrolyte for both experiments. For the purpose of the comparison, CNTs with different morphologies and water plasma treatment times were produced and optimized according to their capacitance performance. Results show that vertically aligned CNTs have improved capacitive performance than random aligned ones and that water plasma treatment cleans the amorphous carbon between nanotubes and increase the capacitance of CNTs from *0.19* to *1* $mFcm^{-2}$. Finally, addition of *2-3 nm* MnO_2 layer on CNTs improve the capacitance significanltly from *1* to *4.5* $mFcm^{-2}$ *(465* Fg^{-1}*)*. Therefore, results demonstrate that MnO_2/MWCNT composite is a promising material to use as an electrode in supercapacitors.**

***Index Terms*- 5. Nanostructure Materials; Manganese oxide, electrochemical deposition, carbon nanotube, supercapacitor.**

I- INTRODUCTION

From their discovery (1991), carbon nanotubes (CNTs) have been an attractive research topic due to their original properties. Although much has been said on CNTs, new applications and new research perspectives are reported every year.

Growing CNTs is normally carried out on a metallic catalyst such as Fe, Ni and Co. From a catalyst layer, after an annealing step, a CNT is grown from each resulting particle being different growing mechanisms possible. Catalyst thickness layer and the diameter of the Fe particles, after annealing, have been correlated with the diameter of the obtained CNTs [1]

Supercapacitors can store electrical energy through two kind of processes, double-layer charging and/or through faradaic process. They fill the gap between batteries (low specific power and high specific energy) and conventional capacitors (high specific power and low specific energy), i.e. they have a specific power as high as conventional capacitors and a specific energy close to that of batteries [2].

Due to their outstanding properties (mechanical, electrical, thermal…), carbon nanotubes (CNTs) have been used in an increasing range of applications. In fact, applications related to supercapacitors have already been reported [3-5]. Nevertheless, the studies carried out on the influence of the morphology (length of CNTs, diameter and alignment) and the properties of functionalization of the CNTs on the supercapacitors efficiency are not determined.

In this work, obtained CNT electrodes were grown by means of plasma enhanced chemical vapour deposition (PECVD) on a catalyst layer deposited by magnetron sputtering. This technology allows us to control diverse parameters such as catalyst thickness layer, temperature and deposition time, which have been optimized to tune CNTs length, diameter and CNT alignment. The obtained CNTs were further modified by plasma post-treatment in order to enhance their electrical response. Finally, a dielectric layer of manganese oxide (MnO_2) was electrochemically deposited on the surface of the CNTs in order to form the supercapacitor structure.

CNTs electrodes were characterized by means of cyclic voltammetry, chronopotentiometry (charge-discharge), Raman spectroscopy, scanning and transmission electron microscopy (SEM, TEM). The two electrochemical methods permit to evaluate the efficiency of the developed electrodes and the SEM and TEM results are used to assess the morphology of the CNTs. In this way, we will be able to correlate the CNTs characteristics with the electrodes ones in view to increase the efficiency of the supercapacitor.

II-OBJECTIVES OF THE WORK

The main objective of this work is to characterize CNT/composite based electrode material to determine the specific capacitance of supercapacitors which directly affects their energy density.

In this purpose, specific objectives were determined for each step of experiment;

a) To study the effects of a water plasma treatment of the obtained CNTs on the specific capacitance of the electrode.
b) Optimization of the electrochemical deposition of MnO_2 on the obtained CNTs.
c) Characterization of the CNTs electrodes in order to determine their electrochemical properties.

III- STATE OF THE ART and MOTIVATION

1. Supercapacitor characteristics, structure and theory

Supercapacitor, also known as electrical double layer capacitor, ultracapacitor, or electrochemical capacitor, is an electrical energy storage device.

Commercial productions of electrochemical supercapacitors in the current markets are based on high surface area porous carbon materials as well as based on noble metal dioxide systems [6]. These commercial supercapacitors are widely used as power sources for activators, or as elements for long time constant circuits, or standby power for random access memory devices, and telephone equipments, etc.

Principle; Supercapacitors have two electrodes immersed in an electrolyte solution, with one separator between them, and two current collectors. The process of energy storage is associated with buildup and separation of electrical charge accumulated on two conducting plates spaced some distance apart as shown in Fig. 1.

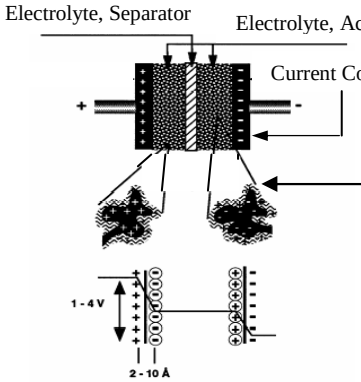

Fig. 1. *Schematic diagram of electric double layer capacitor mechanism and illustration of the potential drop at interface of electrolyte and electrode [7]*

Electrical double layer capacitor accumulates the charge at the interface between the surface of a conductor and an electrolyte solution. When charged, the negative ions in the electrolyte will diffuse to the positive electrode, while the positive ions will diffuse to the negative electrode. In this case, it creates two separated layers of capacitive storage, so the maximum energy density, W, stored in the capacitor is given by equation (1).

$$W = \tfrac{1}{2} C.V^2 \quad (1)$$

where C is the specific capacitance, and V is voltage. The double layer capacitor does not involve chemical reactions, thus supercapacitors have long life cycles of charge and discharge [7]. Some supercapacitors have another contribution to the capacitance associated with reactions at the surface of the electrodes. These reactions consist on electron transfer between the electrolyte and the electrode surface, with the corresponding change in the oxidation state. This kind of capacitance related to faradic processes is referred to as pseudocapacitance.

2. Why to develop a supercapacitor?

Energy storage devices are classified according to energy and power density. Power density is related to the "strength" of a given current and voltage combination, while energy density is related to the duration of time that power can be applied. Electrochemical double layer (ECDL) capacitors are intermediate systems between traditional dielectric capacitors (high power) and batteries (high energy) [6]. A comparison of the properties and performance between battery, capacitor, and supercapacitor is given in Table 1.

Table1. *Comparisons of Capacitor, Supercapacitor and Battery [7]*

Parameters	Capacitors	Supercapacitors	Battery
Charge time	10^{-6} ~ 10^{-3} s	1 ~ 30 s	0.3 ~ 3 hr
Discharge time	10^{-6} ~ 10^{-3} s	1 ~ 30 s	1 ~ 5hr
Energy density (Wh/kg)	< 0.1	1 ~ 10	20 ~ 100
Power density (W/kg)	> 10,000	1,000 ~ 2,000	50 ~ 200
Cyclic life	> 500,000	>100.000	500 ~ 2,000
Charge/discharge efficiency	~ 0.1	0.90 ~ 0.95	0.7 ~ 0.85

Batteries are currently the most common form of electrical energy storage. However, due to their short cycle life and low power densities, batteries are not suitable for many lightweight power source applications [8].

Conventional capacitors also have extended life cycles (i.e., *>10,000*) longer than batteries. However, the small energy density (i.e., *<0.05 Wh/kg*) of capacitors is a significant drawback for many applications which require a large amount of energy storage or delivery [9].

ECDL supercapacitors have properties ranging between these two common energy storage devices.

Supercapacitors offer high power density and long cycle life. Most of available commercial supercapacitors have a specific energy below *10 Wh/kg*. Supercapacitors have higher specific power than batteries and for this reason they are used in conjunction with batteries in power applications. Further improvement of their performance is mainly related to the specific energy. In addition, conventional capacitors are limited by dielectric breakdown. However, supercapacitors typically contain organic electrolytes that may limit their use in some applications [10].

As energy storage devices, supercapacitors could be applied to many emerging technologies such as:

- Electric vehicles,
- Pulse power applications such as satellite propulsion,
- Light rail applications to provide surge power for acceleration,
- Power ride-through circuit, in which a back-up energy cuts in and powers deload if the main power supply fails for a short time. This type generally, dominated by batteries but EDLC are fast making in roads as their price-per-farad, size and effective series,
- Radars and torpedoes in the military domains,
- Defibrillators and cardiac pacemakers in the medical domain,
- Memory supplies in phones or computers.

3. CNTs main characteristics interesting in this case. Why CNTs for Supercapacitors?

The capacitance for an electrochemical device depends on the separation between the charge on the electrode and counter charge in the electrolyte. Since this distance is about few nanometers for nanotubes in electrodes compared to a micrometer in ordinary dielectric capacitors, extremely large capacitances result [9].

There are several reasons why CNT-based electrodes may ultimately be used in supercapacitors. Nanotubes have high electrical conductivity, large specific surface area (*1* to *>2000* m^2/g), good corrosion resistance, high temperature stability, percolated pore structure, small dimensions, a smooth surface topology, perfect surface specificity since only the graphite planes are exposed in their structure and can be functionalized to optimize their properties [9].

Besides, research has shown that CNTs have the highest reversible capacity of any carbon material for use in lithium-ion batteries [11].

4. Growth control of CNTs by PECVD

Today, there are several methods to produce multi wall carbon nanotubes (MWCNTs) such as arc discharge, laser ablation and thermal catalytic chemical vapor deposition (CCVD). Although the two first methods have rapidly known their consecration for the high quality of MWCNTs, their application area appears limited for as-deposited synthesis products [12].

Chemical vapor deposition (CVD) is one of the promising techniques for the growth of CNTs because it makes the growth of nanotubes directly onto substrates possible at relatively low temperature as compared to other techniques such as arc discharge or laser ablation methods.

Radio frequency plasma enhanced CVD (RF-PECVD) is probably the most suitable CNT growth method because it is relatively simple and has a higher reliability than other techniques; it has thus been widely used for thin film deposition in the fabrication of electronic devices. A particular advantage of PECVD for applications in nanoelectronics is that it allows vertically aligned CNT growth at relatively lower temperatures as compared to thermal CVD [13].

5. Metal-oxide deposition techniques and advantages on behavior of supercapacitors

CNT composites have been considered as an effective material for supercapacitor electrodes, the additional phase mainly including electrically conducting polymers and multivalent metal oxide [14]. According to the charge storage mechanism, the addition on the surface of CNT provides an extra capacitance while each tube acts as a micro electrode. They have good chemical stability, good conductivity and a large surface area. In addition, CNTs can be strongly entangled, which provides a network of open mesopores [15]. As a typical representative of metal oxides supercapacitors, RuO_2/CNT composite has shown to possess excellent capacitance performance, but its high-cost and environment harmfulness limit its application. Hence, other compatible metal oxide electrode materials for supercapacitor have been studied extensively, such as NiO, IrO_2, Co_3O_4, and MnO_2. Among them, manganese dioxide exhibits appealing electrochemical properties, such as the rich redox behavior, various structures and oxidation states in electrolyte, which can store and converse the electric charge effectively despite its low cost [14]. Furthermore, the synergistic effects of MnO_2/CNT composites have been employed to improve the poor electric conduction and deficient charge transfer channel of simplex MnO_2 electrodes [14]. Moreover, manganese dioxide is considered environmentally friendlier than other transition metal oxide systems [15].

The routes of general blended processes are difficult in forming homogeneous dispersion of CNT in composite matrix and producing close coating layer of MnO_2 on the surface of CNT. It has been predicted that the uniform MnO_2/ CNT composites can be prepared using the ‘‘redox deposition’’ method [14].

Physical vapor deposition (PVD) layers are rather thin for corrosion protection, and plasma spraying requires sophisticated equipment [16]. Electrochemical deposition offers significant cost, reliability and environmental advantages over the previously used evaporation technology.

In the present work, the possibility of electrochemical deposition (ECD) of MnO_2 onto CNTs was assessed. ECD can accommodate the whole range of different length scales found on a large *200 mm* or *300 mm* diameter wafer. Amorphous-$MnO_x{\cdot}nH_2O$ films were deposited on the CNTs by anodic deposition [5].

6. Characterization techniques interesting in this case

In our work, characterization was made considering two different goals according to the purpose of the study. First one is electrochemical characterization and second one is microscopic and spectroscopic characterization.

For the electrochemical techniques, cyclic voltammetry was performed to interpret supercapacitor behavior of CNTs electrode after and before MnO_2 deposition. Besides, galvanostatic charge-discharge was made to see the discharge behavior and to calculate the specific capacitance of CNTs electrode after and before MnO_2 deposition.

6.1. Electrochemical Characterization Techniques

Cyclic Voltammetry;

In typical cyclic voltammetry (CV), a solution component is electrolyzed (oxidized or reduced) by placing the solution in contact with an electrode surface, and applying a sufficiently positive or negative voltage to the electrode. In simple cases, the surface is started at a particular voltage with respect to a reference half-cell such as calomel or Ag/AgCl electrode, the electrode voltage is changed to a higher or lower voltage at a linear rate, and finally, the voltage is changed back to the original value at the same linear rate. When the surface becomes sufficiently negative or positive, a solution species may gain electrons from the surface or transfer electrons to the surface, respectively. This results in a measurable current in the electrode

circuitry. When the voltage cycle is reversed, it is often the case that electron transfer between electrode and chemical species will also be reversed, leading to an "inverse" current peak [17]. These features are illustrated in Fig. 2.

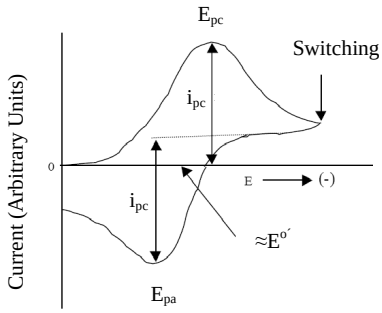

Fig. 2. *Shape of a voltammogram for a Nernstian electrochemical reaction [17] (Epa is the potential of the anodic current, Epc is the potential of the cathodic current)*

The quantitative simulations show several things for a Nernstian system. The peak current in a cyclic voltammogram containing only one species is described by the Randles-Sevcik equation:

$$i_p = 0.4463 n \cdot F \cdot A \cdot C \left(\frac{n \cdot F \cdot \nu \cdot D}{R \cdot T} \right)^{1/2} \quad (2)$$

$$i_p = \left(2.69 \times 10^5\right) n^{2/3} \cdot A \cdot D^{1/2} \cdot \nu^{1/2} \cdot C^*$$

At *25 ^oC* where *F* is Faraday's constant (*96485 C / mol*), *R* is the universal gas constant (*8.314 J / mol K*), i_p is the peak current in *A*, *n* is the number of electrons transferred, *A* is the electrode active surface area in cm^2, *D* is the diffusion coefficient of the species in cm^2/s, *v* is the scan rate in Vs^{-1} and *C** is the bulk concentration of the species in mol/cm^3 [17]. From this equation, it is possible to obtain electrode active surface area "*A*".

The achievement of rectangular-shaped cyclic voltammograms over a wide range of scan rates is the ultimate goal in electrochemical double-layer capacitors [18]. Because the bigger area inside the CV curves refers to bigger capacitance of electrode. This behavior is very important for practical applications. First, a higher energy density is expected, because the usable potential range is wide. Second, a higher power density is expected as the critical scan rate increases

Charge Discharge;

Galvanostatic charge/discharge is a more reliable method for getting the specific capacitance than CV [19]. All charge/discharge curves should be almost linear and symmetric like in Fig. 3.

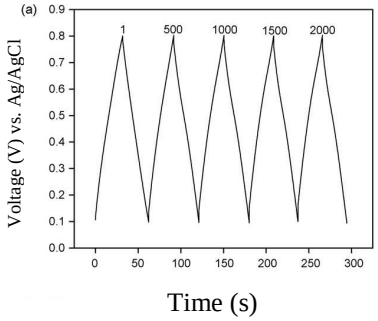

Fig. 3*. Charge–discharge curve vs. time.[20] The numbers at top of the curves refer to the cyclic time.*

The specific capacitance is calculated from the liner part of charge/ discharge curves using:

$$C = I / [(\Delta V/\Delta t).A] \quad (3)$$

Where *I* is the constant current, Δt is the time interval for charge/ discharge in voltage ΔV, *A* is the active surface area of composite material and *C* is specific capacitance [19].

6.2. Microscopic and Spectroscopic Techniques

For the microscopic and spectroscopic characterization; first Raman spectroscopy was performed to observe the chemical composition of obtained electrode after water plasma treatment. Also scanning electron microscopy (SEM) was made; to check the growth of CNTs; to check the homogeneity of CNTs tips and the presence of amorphous carbon, to see the MnO_2 on CNTs. Last, transmission electron microscopy (TEM) was made to check the presence and thickness of MnO_2 on the surface of CNTs.

Raman Spectroscopy;

Raman spectroscopy is a spectroscopic technique used to study vibrational, rotational, and other low-frequency modes in a system [21].

The structure, topology, and size of CNTs are a source of their outstanding mechanical and optical properties and their electronic behavior. Raman spectroscopy is a popular technique for determining the diameter distribution, chirality, purity, and architecture of CNTs.

The most prominent Raman features in CNTs are the radial breathing modes (RBMs), the higher frequency *D* (disordered), *G* (graphite), and *G'* (second-order Raman scattering from *D*-band variation) modes. The quality of a sample has often been evaluated using the *D*/*G* band intensities. For high-quality samples without defects and amorphous carbon, the *D*/*G* ratio is often less than *2 %* [22].

Scanning Electron Microscopy;

The scanning electron microscope (SEM) is a microscope that uses electrons rather than light to form an image. The SEM also produces images of high resolution, which means that closely spaced features can be examined at a high magnification. The combination of higher magnification, larger depth of focus, greater resolution, and ease of sample observation makes the SEM one of the most heavily used instruments in research areas today [23].

Transmission Electron Microscopy;

The transmission electron microscope (TEM) operates on the same basic principles as the light microscope but uses electrons instead of light. What you can see with a light microscope is limited by the wavelength of light. Also their much lower wavelength makes it possible to get a resolution a thousand times higher than with a light microscope [24].

IV- METHODOLOGY

1. Preparation of CNT-based electrode

CNT based electrode production was carried out in a reactor resulting from the European project "Nanotube" (Fig. 4).

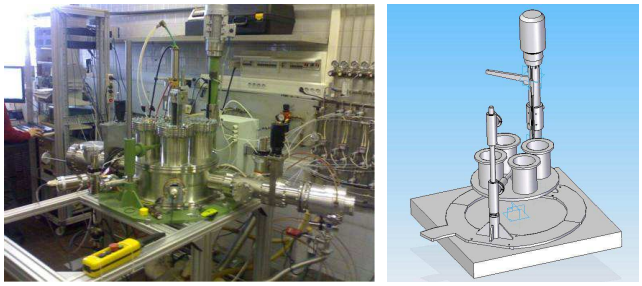

Fig. 4. *PECVD reactor and Lift system to open [26]*

This reactor consists on three magnetron sputtering heads and a high temperature PECVD accessory. All these process heads mounted in the same chamber (reduction of manufacture costs and power consumption) and with a simple "Turn-on" procedure of the whole system, there is an easy maintenance and no time consuming during processes. This reactor enables the possibility of biasing the substrate and high vacuum conditions [25].

During the processes, all parameters were controlled by using a PC software control in "Labview" of NI

CNT based electrode production procedure was carried out according to Fig. 5, which shows the whole performed processes to optimize operating conditions in order to obtain better CNT based electrodes.

During production of CNT based electrode, to make an optimization, SEM was used to: *i)* find the optimal annealing temperature in order to obtain a desired formation of Fe particles to growth CNTs; *ii)* assess vertical alignment, and homogeneity of the deposited CNTs and; *iii)* evaluate water plasma effect on the CNT morphology.

In accordance with these purposes; sputtering of Fe catalyst on Si wafer was use to deposit *3 nm* with the presence of *2 Pa* and *50 W* Ar plasma. PECVD was chosen as a better process to grow vertically aligned CNTs. Growth process with PECVD was done at *680 °C*, *900 s* and *50 W* RF power in the presence of NH_3/C_2H_2 mixture where NH_3 is using as a carrier gas and C_2H_2 is a precursor gas.

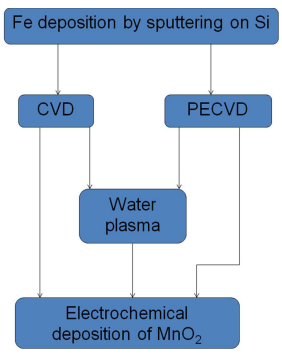

Fig. 5*. Algorithm of making CNT based electrode*

The water plasma helps to open the ends of CNTs to make the inner side functional and also to remove amorphous carbon from the CNTs. Avoiding amorphous carbon makes the area between CNTs area clean and functional where the ion diffusion also happens. Besides, opened tips permit to the inside of the wall of CNTs to be functional. Therefore, this effect provides higher surface area.

Time and pressure parameters are the most important ones which can change the growth of CNTs significantly. As a result, water plasma was performed at *50 Pa* and *60 s* with *50 W* plasma power. The details of optimization can be found in Burak Caglar's thesis [26]. Then the metal-oxide deposition was made by electrochemical deposition using three electrode e-cell system. To change the thickness some parameters have been optimized like: concentration of electrolyte solution, deposition time and voltage during electrochemical deposition.

2. Design and construction of experimental setup and description of general system of 'AutoLab'

Both MnO_2 deposition and electrochemical measurement were carried out inside the same homemade electrochemical cell (Fig. 6-a). The cell has a volume of *500 ml* and consists of three input holes used to introduce the different electrodes; counter electrode, Ag/AgCl reference electrode and working electrode.

AutoLab (PGSTAT30, USA, Fig. 6-b) system was used for the electrochemical deposition of MnO_2 and for the electrochemical characterization of the samples.

Systems setup was almost the same for both MnO_2 deposition and electrochemical measurements. After putting the electrolyte inside the e-cell, it is mixed by using a magnetic twister below the e-cell. In this way electrolyte can be kept homogeneous inside the e-cell.

The cell is provided with a gas entrance that allows the removal of oxygen by bubbling nitrogen gas through the solution (Fig. 7). The setup also allows the magnetic stirring of the aqueous solution.

3. Metal-Oxide Deposition

Manganese oxide deposition was carried out in the three electrode e-cell system (Fig. 6-a) by applying an anodic potential to the CNTs electrode using a Pt ring electrode as the counter electrode and a Ag/AgCl reference electrode in a Mn_2SO_4 solution. AutoLab system device was used for the electrochemical deposition and all parameters were controlled by using Nova 1.5 (Copyright 2009, Eco Chemie B.V.) software.

Fig. 6. *a) Three electrode e-cell system b) AutoLab System*

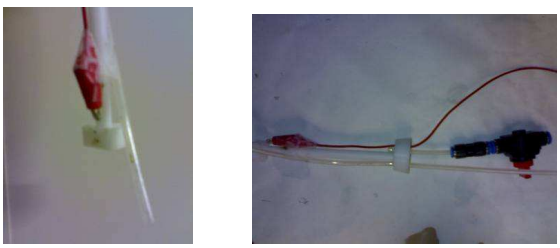

Fig. 7*. Working electrode holder system used inside e-cell.*

Before deposition process, deposition conditions such as applied potential, aqueous solution of MnO_2 concentration were defined according to the previous studies. In this way, parameters were fixed such as: concentration of solution *0.2 M* Mn_2SO_4 and set potential: *0.4 V*. Then, to calibrate the deposition rate of MnO_2, *30 min* deposition time was performed on a Si wafer to be able to measure the thickness by using Atomic Force Microscopy (AFM). Then three different MnO_2 deposition time '*3 min, 6 min*, and *10 min*' were tested and the capacitance of the obtained samples was measured in order to assess the influence of MnO_2 on the final properties of the electrode.

4. Characterization techniques

As described in section III-6, CV, charge discharge, Raman spectroscopy, SEM and TEM were performed to characterize MnO_2/MWCNTs composite electrode material.

4.1. Electrochemical Characterization

CV and charge-discharge behavior were utilized to evaluate the electrochemical behaviors of the MnO_2/MWCNT composite.

The main role of the CV was to see the redox behavior and compare capacitance calculating the area inside the curve. CV is also used to determine the active surface area of the CNTs electrodes by introducing the sample in a solution with an electrolyzable species (Fe^{2+}/Fe^{3+}). In charge-discharge experiments, the discharge behavior was observed and using equation (3) the specific capacitance of the CNT based electrode was obtained. The MnO_2/CNT composite with a definite area of about *1* cm^2 was used as working electrode. A commercial Metrohm Pt ring electrode served as the counter electrode, and Ag/AgCl was used as a reference electrode to control the potential of the working electrode. A *0.2 M* Na_2SO_4 solution was used as electrolyte, respectively. Additionally, *0.005 M* $KFe(CN)_6$ with *0.1 M* Na_2SO_4 solution was used to determine the surface area of CNTs. Active surface area, *A*, was calculated using equation (2).

All electrochemical experiments were carried out at room temperature and the potentials were referred to a Ag/AgCl reference electrode. All chemicals were analytic grade. Double-distilled water was used throughout.

4.2. Microscopic and Spectroscopic Characterization

The morphologies of the MnO_2 film and MnO_2/CNT electrodes were observed by SEM (FESEM, Hitachi S-4100, Japan). This technique was also used to optimize the parameters that affect the morphology of the CNTs during the production process such as; annealing temperature, annealing time, plasma power and water plasma treatment. The nanostructure of the MnO_2/CNT electrode such as thickness, homogeneity and the nanostructure of CNTs such as SW or MW CNTs were examined using TEM (CM-30, JEOL, Holland). The characterization of water plasma effect on amorphous carbon was done based on Raman Spectroscopy (T 64000, Jobin Yvon, Division Instruments (ISA), Japan).

VI- RESULTS and DISCUSSION

1. CNTs morphology influence on supercapacitor properties

By producing vertically aligned CNTs on Si electrode, we obtain a potentially higher active surface area than in random aligned CNTs. Therefore, higher active surface area will provide higher ion transfer and capacitance for supercapacitors.

Fig. 8 shows the morphological differences between three samples of CNTs obtained under different conditions. The desired CNTs (Fig. 8-a) have vertical and homogeneous alignment with high density while the other CNTs (Fig 8-b and c) showed random and less dense alignment. Table 2 shows the properties and the growth conditions of these three CNTs samples.

To be able to make a calculation of active surface area, current vs. potential curve was obtained in a *0.005 M* $KFe(CN)_6$ *1 M* Na_2SO_4 solution. Using equation (2), the obtained active surface areas were 3.92 ± 0.1, 1.04 ± 0.02 and 1.52 ± 0.044 cm^2 for the vertically aligned CNTs electrode and other two random aligned CNTs electrodes. Fig. 9-b indicates the current vs. scan rate curve which was obtained from CV graph (Fig. 9-a) to calculate the active surface area from slope of the line.

Cyclic voltammetry comparison measurements of same three samples are shown in Fig. 10 to compare the redox behavior and capacitance performance. Vertical and high densely CNTs show higher redox ad capacitive behavior than other CNTs. From the charge-discharge measurements, the following specific capacitances of the CNTs tested electrodes were obtained using equation (3); *0.19, 0.11* and *0.13* $mFcm^{-2}$ in orderly for Fig. 8-a, b and c.

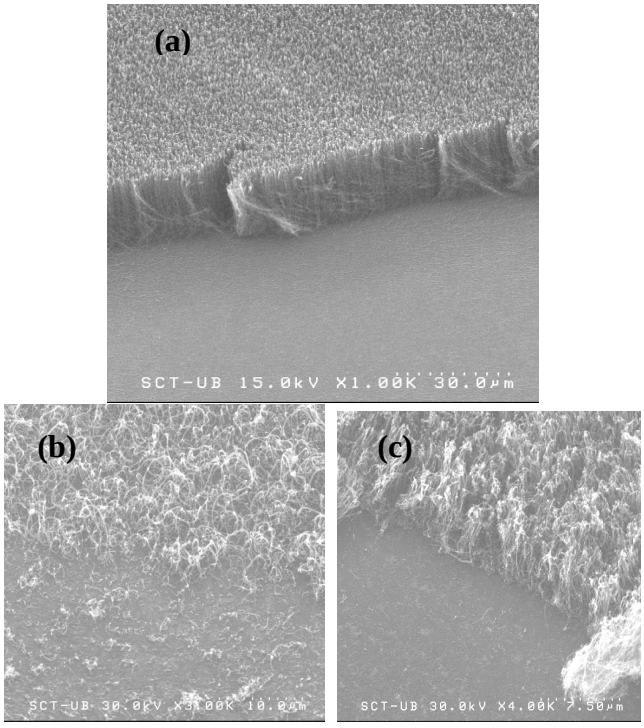

Fig. 8. *SEM images of CNT growth type obtained in three different conditions a) 3 nm Fe thickness, 680 °C PECVD, b) 5 nm Fe thickness, 750 °C PECVD, c) 5 nm Fe thickness, 680 °C PECVD*

***Table2**. Conditions and results of different CNTs samples*

#	CNTs diameter(nm)	CNTs Length (µm)	Immersed Area (cm^2)	Active surface Area (cm^2)	Active Surface Area / Immersed Area	Specific Capacitance ($mFcm^{-2}$)
3 nm Fe, 680 °C PECVD	21	15.8	0.64	3.92 ± 0.1	6.13	0.19
5 nm Fe, 750 °C PECVD	95	3.8	1.43	1.04 ± 0.02	0.73	0.11
5 nm Fe, 680 °C PECVD	81	3.9	1.08	1.56 ± 0.05	1.44	0.13

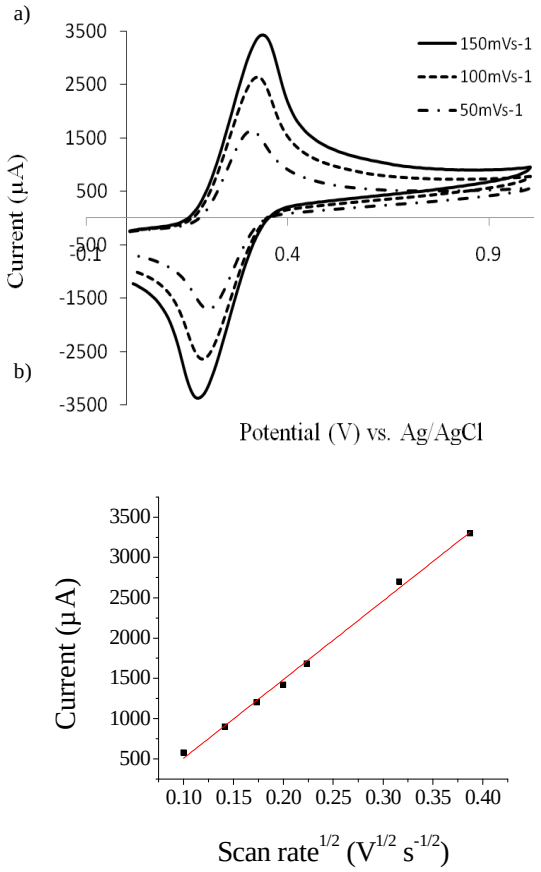

***Fig. 9.** a) CV results of VA- CNTs with applying 3 different scan rate (50, 100 and 150mVs^{-1}), b) Current vs. scan rate curve obtained from previous figure*

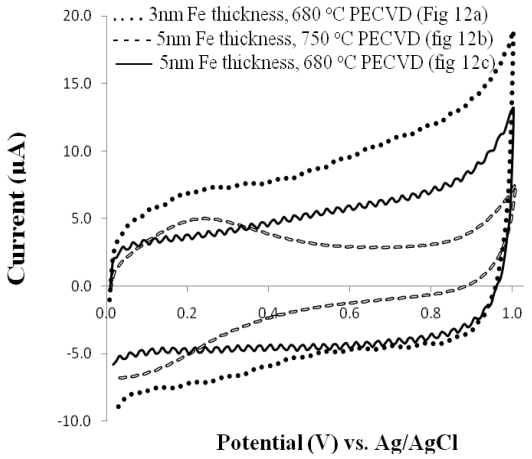

***Fig. 10.** Cyclic voltammetry results of samples with 150mV s^{-1} scan rate.*

As we can clearly see from the Table 2 and SEM images, at low temperature, CNTs density is always higher than at high temperature, so when using PECVD, high temperature process does not provide enough alignment and high dense CNTs. From Table 2 results we can conclude that, vertically aligned CNTs have better specific capacitance than random aligned one. In fact, we can also conclude that, as expected, the specific surface area is larger when the CNTs are vertical and thinner.

2. Water plasma influence on supercapacitor properties

Water plasma was done to remove amorphous carbon from the CNTs samples. Moreover, water plasma helps to open ends of CNTs to make the inner side available. Time and pressure parameters can be changed in order to optimize the water plasma process. The morphology and the amorphous carbon contamination were changed with performing water plasma on CNTs.

Water plasma conditions were first optimized according to their effect on amorphous carbon. *60 s* water plasma showed a clearer effect if compared to other conditions (*30 s* and *300 s*). SEM and TEM images show the effect of water plasma clearly, as shown in Fig. 11. Fig. 11a-I indicates the CNTs without water plasma while Figure 11a-II shows CNTs after *60 s* water plasma. Diameter of CNTs also decreases from *21 ± 3* to *15 ± 2* with water plasma conditions, as shown in TEM figures, Fig. 11-b**.**

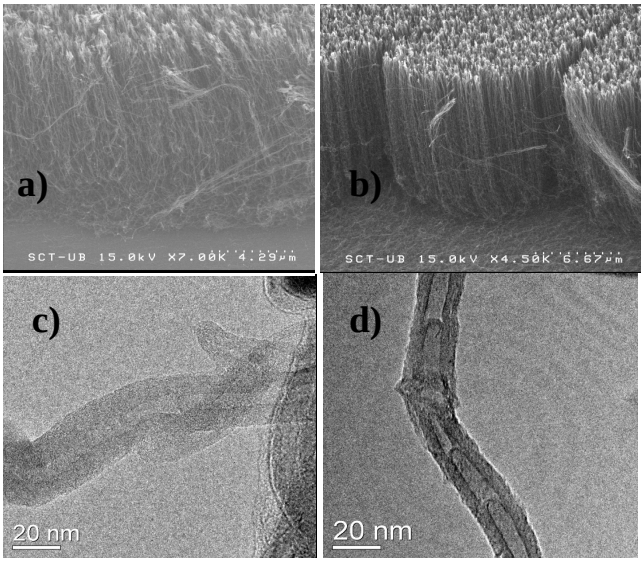

***Fig. 11**. SEM iamges and TEM images of CNTs a) and c) without water plasma, b) 60 s and d)300 s water plasma*

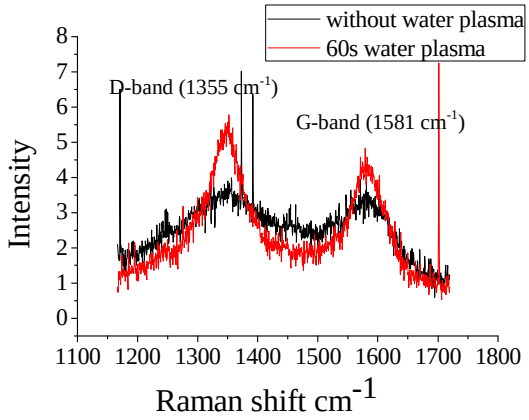

Fig. 12. *Raman spectroscopy of 60s water plasma CNTs compared to an un-treatment sample ones*

The main features in the Raman spectra are first-order ones. The so-called disorder-induced *D* band appears at *1355 cm^{-1}* and *G* band appears at *1581 cm^{-1}* in the MWNT sample spectra, like in the Fig. 12.

The most distinct characteristic of first order amorphous carbon Raman spectrum is an asymmetric feature in the *1000 - 1800 cm^{-1}* with the summit at about *1450 cm^{-1}*. Fig. 12 shows the Raman spectrum of two CNT electrode sample. As is seen from the water plasma curve, the amount of the amorphous carbon obviously decreased after performing *300 s, 50 W* water plasma at room temperature and *50 Pa*. Also the presence of amorphous carbon affects the Raman spectrum of MWCNTs and display the *D* and *G* band in low intensities, as is seen from without plasma curve.

The active surface area of CNTs decreased from *3.92* to *1.04 cm^{-2}* after a *60 s* water plasma treatment. It can be related with the decreasing in the diameter of CNTs after plasma implementation. Fig. 13-a shows the obtained CV of CNTs after *60 s* water plasma in 0.005 M $KFe(CN)_6$. 1 M Na_2SO_4 solution with applying three different potential rates (*50, 100* and *150 mVs^{-1}*). Fig. 13-b indicates the current vs. scan rate curve which is obtained from CV graphs (Fig. 13-a) to calculate the active surface area from slope of the line.

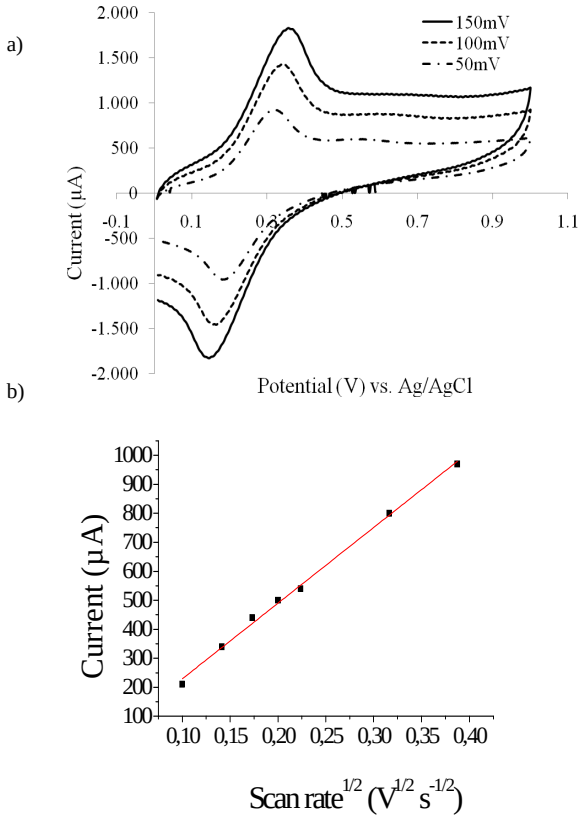

Fig. 13. *a) CV 60 s water plasma CNTs with applying 3 different scan rates (50, 100 and 150 mVs^{-1}), b) Current vs. scan rate curve obtained from previous figure*

Cyclic voltammetry results shown in Fig. 14, prove that water plasma improve capacitive performance due to the removal of the amorphous carbon. Applying *60 s* water plasma, the specific capacitance showed a raise from *0.19* to *1 $mFcm^{-2}$* according to their charge-discharge results obtained using equation (3). But on the contrary, too long or too short plasma negatively affects the specific capacitance (*0.48 $mFcm^{-2}$* for *300 s* water plasma, *0.32 $mFcm^{-2}$* for *30 s* water plasma) since the plasma makes the CNTs shorter or does not clean the amorphous carbon enough. Fig. 14 also proved that with *60 s* plasma shows higher capacitance compared not only to the CNTs without plasma but also to the other plasma times (*30* and *300 s*).

Table 3*. Conditions and results of CNTs with different water plasma*

#	Diameter (nm)	Length (nm)	Immersed Area (cm^2)	Active Surface Area (cm^2)	Active Surface Area / Immersed Area	Specific Capacitance ($mFcm^{-2}$)
without water plasma	21 ± 3	15.8	0.64	3.92 ± 0.1	6.13	0.19
30s water plasma	30 ± 4	9.0	1.05	1.28 ± 0.03	1.22	0.32
60s water plasma	15 ± 2	11.2	0.49	1.04 ± 0.02	2.12	1
300s water plasma	17 ± 2	5.5	0.8	1.48 ± 0.09	1.85	0.48

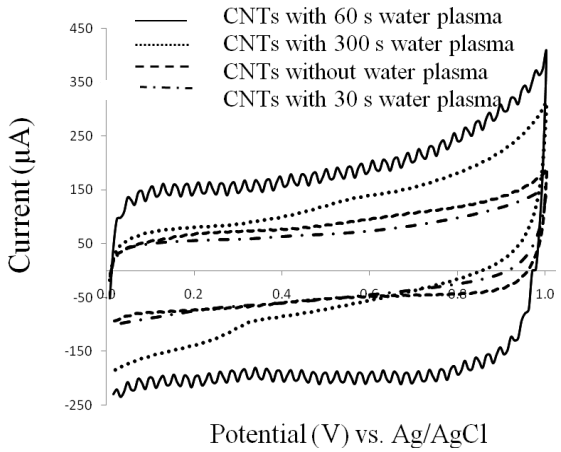

Fig. 14 *CV of CNTs without and with different water plasma times in 150 mVs^{-1} scan rate.*

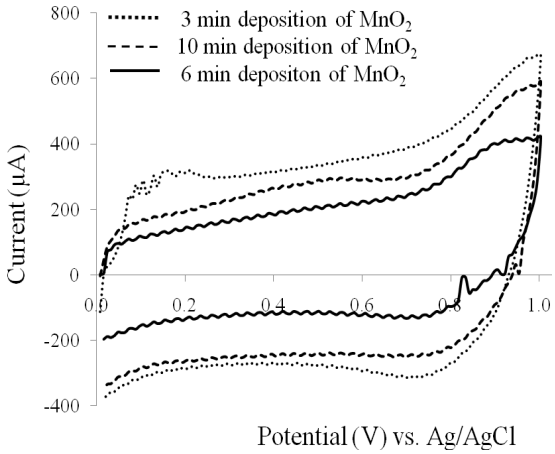

Fig. 15. *Cyclic voltammetry compare of three different MnO_2 deposited time CNT electrodes in 150mVs^{-1} potential scan rate*

Figure 14 also indicates that, there is no significant capacitance performance difference with applying *30 s* water plasma to CNTs. But applying *300 s* water plasma shows better capacitance performance compared to *30 s* water plasma. Therefore, we can conclude that even with shorter CNTs, long time water plasma shows higher capacitance thanks to the more open surface and less amorphous carbon contamination. And also we can say that the removal of amorphous carbon has more significant effect to capacitance than the length of CNTs.

Table 3 indicates that, performing water plasma after the growth CNTs is a suitable option to remove the amorphous carbon from the samples and it increases their specific capacitance.

So we can conclude that the implementation of water plasma increases the specific capacitance of electrode, thanks to more open and higher active surfaces of CNTs by removing the amorphous carbon contamination, as shown in the substrate part of Figure 11 a-II.

3. Manganese oxide influence on supercapacitor properties

3.1. Determination of solution composition

After several trials of different conditions, deposition rate of MnO_2 could not be found on CNTs. However, the deposition rate on a Si wafer was determined by measuring the thickness of the deposited MnO_2 layer with AFM for different deposition times. From these studies the deposition rate was taken as *1 nm* MnO_2 thickness per minute in a *0.2 M* Mn_2SO_4 solution applying a voltage of *0.6 V* [27].

3.2. Optimization of deposited thickness

To make an optimization of MnO_2 deposited thickness, three different thicknesses were tried such as *3, 6* and *10 nm* which corresponds to the deposition times; *3, 6* and *9 min*, respectively. CV curves indicate that the best capacitance is obtained after *3* minutes of deposition time (Fig. 15).

The presence of MnO_2 film for *3 min* deposition can be seen from SEM and TEM images, Fig. 16.

According to the SEM images, MnO_2 layer seems well deposited not only on the tips but also on the lateral surfaces of CNTs. Also in these images, lots of gaps were seen on the surface and these may cause from the hidrophobicity of CNTs in the aqueous solution.

From TEM images, thickness of MnO_2 layer was found to be *2.4 ± 0.4 nm* for *3 min* deposition. It proves that the deposition rate is approx. *0.8 ± 0.1 nm/min* which is close to the value that we estimated before.

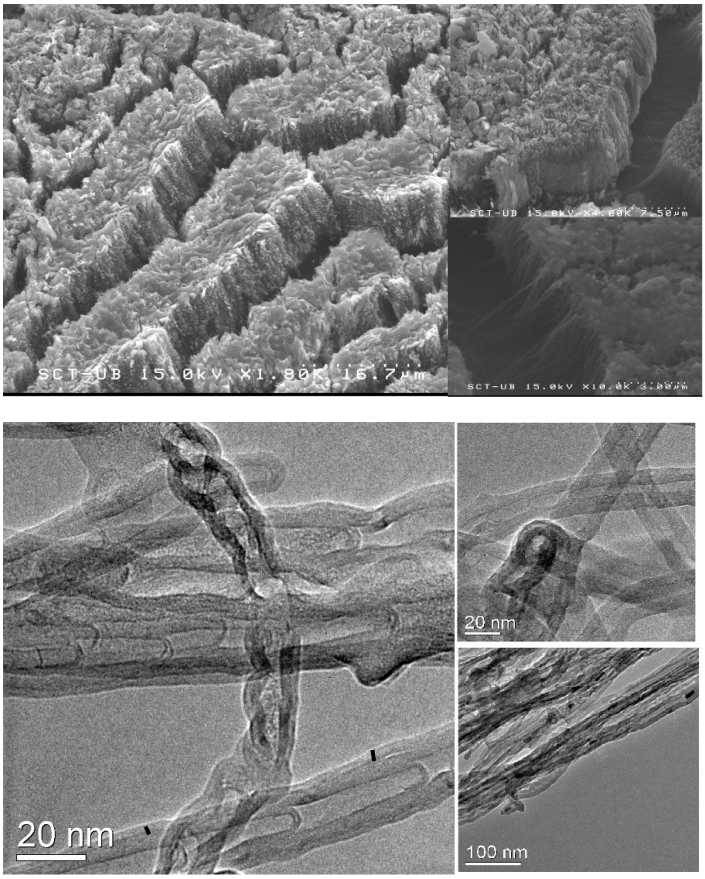

Fig. 16*. SEM and TEM images of MnO_2 deposited CNTs after 3 min deposition. MnO_2 layer can be seen in TEM figures.*

Table 4 *Conditions and results of CNT electrode functionalization*

#	Diameter (nm)	Length (nm)	Immersed Area (cm^2)	Surface Area (cm^2)	Immersed Area / Active Surface Area	Specific Capacitance ($mFcm^{-2}$)
VA-CNTs	21 ± 3	15.8	0.64	3.92 ± 0.1	6.13	0.19
VA-CNTs, 60 s water plasma	15 ± 2	11.2	0.49	1.04 ± 0.022	2.12	1
VA-CNTs, 60 s water plasma, 3 nm MnO_2 layer	24 ± 3		0.55	0.36 ± 0.02	0.65	4.5

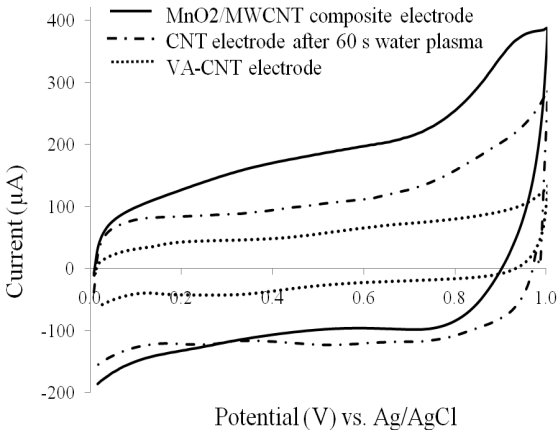

Fig. 17*. CV results compare of three different sample of three different condiiton at 100mVs^{-1} scan rate*

Finally, Fig. 17 shows that MnO_2 layer increased the specific capacitance of CNT electrode significantly. It was found that with *3 nm* MnO_2 deposition on CNT electrode, the specific capacitance increase from *1* to *4.5* $mFcm^{-2}$ (*1* $mFcm^{-2}$ corresponds to CNTs with *60 s* water plasma). Also from Table 4, it can be seen that the increase of specific capacitance for different functionalization processes.

Specific capacitance for MnO_2/MWCNT electrode was also found in Fg^{-1}. It was estimated that all Mn^{2+} was oxidized to Mn^{4+} during electrochemical deposition. And the total mass of MnO_2 was determined according to the total charge that passed through the electrode during this oxidation and using Faraday constant and the molar mass of MnO_2 (*3.5 x* 10^{-6} *g*).

Finally, the specific capacitance of the MnO_2/MWCNT electrode was found to be *463* Fg^{-1}.

Table 5 shows the different specific capacitance results and the conditions. Highest value has been obtained by K.-W. Nam et al. [37] as *1701* Fg^{-1} using NiO_x/MWCNT composite material on Si wafer. Also, C. Fang and coworkers have obtained *1380* Fg^{-1} with RuO_2/MWCNT composite material on Si wafer [32].

MnO_2/MWCNT composite material was also studied on several materials [14, 20, 28, 30, 31, 33, 36, 38, 39, 41]. The highest value using MnO_2/MWCNT material has been obtained by Z. Fan et al. as *579* Fg^{-1} on graphite substrate [35]. In the closest study with our work, Kyung-Wan Nam and coworkers have obtained *471* Fg^{-1} by using MnO_2/MWCNT material on Si wafer [31].

CONCLUSIONS

As it was indicated before, CNTs are good conductive, high specific area materials well suited to supercapacitors requirements. Besides and more importantly, their surface can be functionalized by metal oxide, polymers or oxidizing to overcome the presence of some impurities.

Our work showed that the appropriate materials and processes can be optimized to improve the CNT capacitance performance which can be used in energy devices.

In the first step, we obtained that vertically aligned CNTs have higher capacitance than random ones so it proves that the morphology affects capacitance significantly. Because, even when the CNTs are dense and long, they don't have as high specific capacitance as with vertically aligned CNTs.

The surface treatment of the CNTs with water plasma was proven to give higher results thanks to the clearer and larger active surfaces of nanotubes. Long time water plasma did not show higher capacitance despite of the remaining amorphous carbon contamination because when the plasma time becomes longer, plasma starts to cut the tips of the nanotubes and makes them shorter and also smaller in diameter.

MnO_2 addition was the crucial step and process for our work and we obtained the highest specific capacitance of, *475* Fg^{-1} with a *3 nm* MnO_2 layer.

So it was proved that MnO_2/MWCNT is very suitable and strong material to use as an electrode in a supercapacitor. And that MnO_2 is an effective, low cost composite material.

ACKNOWLEDGMENTS

A.T. Mutlu thanks to Prof. Enric Bertran, Dr. Eric Jover Comas, Dr. Roger Amade Rovira and Dr. Carles Corbella Roca for their guidance and helps in every step of this work and to technicians in Serveis Científico-Tècnics of the Universitat de Barcelona (SCT-UB) for measurement facilities. Also special thanks to my coworker Burak Caglar for his help and hard work during all steps of project. This work was supported by the Generalitat de Catalunya (Projects 2005SGR00666 and 2009SGR00185) and the MEC of Spain (Projects DPI2006-03070 and MAT2009-14674-C02-01).

***Table 5**. Specific Capacitance Results and process conditions of other studies*

Ref. no	Electrode material	CNT morph.	CNT diameter	Composite material/deposition tech.	Spec. Cap.
[28]	Polished graphite plates	MWCNT	10–20nm	PSS/PEDOT/MnO_2	375F/g
[29]	Si wafer	MWCNT		RuO_2(electrochemically deposited)	1170 F/g
[30]	Nickel foam	MWCNT	15nm	Manganese dioxide nanofibers	155 F/g
[31]	Si wafer	MWCNT	15 to 40 nm	MnO_2(electrodeposition)	471 F/g
[32]	Si wafer (Ti film 200 nm)	MWCNT		RuO_2	1380 F/g
[33]	Ni foam		20 nm	MnO_2	522 F/g
[14]	Ni foam	MWCNT		MnO_2(in situ coating)	250.5 F/g
[34]	Graphite	MWCNT		RuO_2	628 F/g
[20]	Ti foil	MWCNT	20nm	MnO_2(coprecipitation method)	250 F/g
[35]	Si wafers	MWCNT		Polypyrole (PPy)	250 F/g
[36]	Graphite substrate	MWCNT	50-100 nm	γ-MnO_2 (electrochemically induced deposition)	579 F/g
[37]	Si wafer	MWCNT		NiOx (electrochemical deposition)	1701 F/g
[38]	Graphite substrate	MWCNT		Mn-oxide (electrophoretic deposition technique, EPD)	260 F/g
[39]	Stainless-steel	MWCNT	70–80 nm	Manganese dioxide (electrodeposition)	356 F/g
[40]	Ni-foam	MWCNT	30-70 nm	Nickel oxide	160 F/g
[41]	Platinum foil	MWCNT	50-100 nm	MnO_2 (thermally decomposing manganese nitrates)	568 F/g

REFERENCES

[1] Eric Jover, Burak Caglar, Toygan Mutlu And Enric Bertran, "*Description Of CNTs Intercalated Structures Obtained by CVD*", TNT2009 Conference, September 2009

[2] Peng, C., Zhang, S., Jewell, D., Chen, G.Z., "*Carbon nanotube and conducting polymer composites for supercapacitors*", Progress in Natural Science, **18** (2008)777-788

[3 Chen, J.H., Li, W.Z., Wang, D.Z., Yang, S.X., Wen, J.G, "*Electrochemical characterization of carbon nanotubes as electrode in electrochemical double-layer capacitors*", Carbon, **40** (2002)1193-1197

[4] Li, C.S., Wang, D.Z., Liang, T.X., Wang, X.F, "*A study of activated carbon nanotubes as double-layer capacitors electrode materials*", Materials Letters, **58** (2004) 3774-3777

[5] Lee, C.Y., Tsai, H.M., Chuang, H.J., Li, S.Y., Lin, P., Tseng, T.Y., "*Characterization and electrochemical performance of supercapacitors with manganese oxide-carbon nanotube nanocomposite electrode*", Journal of the Electrochemical Society, **152** (2005) A716-A720

[6] B. E. Conway, "*Electrochemical supercapacitors, scientific fundamental and technological applications*", Plenum Publishers, 1999

[7] Chongfu Zhou, "*Carbon nanotube based electrochemical supercapacitors*", Georgia Institute of Technology, Atlanta, December, 2006

[8] http://data.energizer.com/PDFs/typical_characteris tics.pdf

[9] J.M. Boyea, R.E. Camacho, S. P. Turano, W. J. Ready, "*Carbon nanotube-based supercapacitors: technologies and markets*", Nanotechnology Law & Business, March 2007

[10] V.V.N. Obreja, "*On the performance of supercapacitors with electrodes based on carbon nanotubes and carbon activated material—A review*", Physica E **40** (2008) 2596-2605

[11] M. Paradise, T. Goswami, "*Carbon nanotubes-production and industrial applications*", Materials and Design **28** (2007) 1477-1489

[12] A. Gohier, T.M. Minea, A.M. Djouadi, A. Granier, M. Dubosc, "*Limits of the PECVD process for single wall carbon nanotubes growth*", Chemical Physics Letters **421** (2006) 242-245

[13] Hideki Sato, Takamichi Sakai, Atsushi Suzuki, Kazuo Kajiwara, Koichi Hata, "*Growth control of carbon nanotubes by plasma enhanced chemical vapor deposition*", Vacuum **83** (2009) 515-517

[14] X. Xie, L. Gao, "*Characterization of a manganese dioxide/carbon nanotube composite fabricated using an in situ coating method*", Carbon **45** (2007) 2365–2373

[15] Sang-Bok Maa, Kyung-Wan Nam, Won-Sub Yoon, Xiao-Qing Yang, Kyun-Young Ahn, Ki-Hwan Oh, Kwang-Bum Kim, "*Electrochemical properties of manganese oxide coated onto carbon nanotubes for energy-storage applications*", Journal of Power Sources **178** (2008) 483–489

[16] Knörnschild, G, 2005, "*Electrophoretic deposition of aluminum on an Mg-Alloy*", Revista Matéria, **10**, n. 3, pp. 497 – 501

[17] http://www.earlham.edu/~chem/chem341/c341_labs_web/ cyclic_voltammetry.pdf

[18] J.H. Chen, W.Z. Li, D.Z. Wang, S.X. Yang, J.G. Wen, Z.F. Ren, ´´*Electrochemical characterization of CNT as electrode in electrochemical double-layer capacitors*´´ Carbon, **40** (2002) 1193– 1197

[19] Chen Ye, Zhang Mi Lin, "*Electrochemical and capacitance properties of rod-shaped MnO_2 for supercapacitor*" Journal of The Electrochemical Society, **152** (2005) A1272-A1278

[20] J.M. Ko, K.M. Kim, "*Electrochemical properties of MnO2/activated carbon nanotube composite as an electrode material for supercapacitor*", Materials Chemistry and Physics **114** (2009) 837–841

[21] http://en.wikipedia.org/wiki/Raman_spectroscopy

[22] http://www.youngin.com/application/CNT.pdf

[23] http://mse.iastate.edu/microscopy/whatsem.html

[24] http://nobelprize.org/educational_games/physics/microscopes /tem/index.html

[25] J. García-Céspedes, S. Portal, A. Canillas, E. Pascual, E. Bertran, European Project, Departament de Física Aplicada i Òptica, Universitat de Barcelona, 2007

[26] Burak Caglar, "Production of Carbon Nanotubes by PECVD for supercapacitor applications", Thesis of Master, Universidad de Barcelona, Barcelona, 2010

[27] C.Y. Lee, H.M. Tsai, "*Characteristics and electrochemical performance of supercapacitors with manganese oxide-carbon nanotube nanocomposite electrode*", Journal of the Electrochemical Soc., **152**(4) (2005) A716-A720

[28] R.K. Sharma, L. Zhai, "*Multiwall carbon nanotube supported poly(3,4-ethylenedioxythiophene)/ manganese oxide nano-composite electrode for super-capacitors*", Electrochimica Acta **54** (2009) 7148-7155

[29] Il-Hwan Kim, Jae-Hong Kim, Young-Ho Lee, and Kwang-Bum Kima, "*Synthesis and characterization of electrochemically prepared ruthenium oxide on carbon nanotube film substrate for supercapacitor applications*", Journal of The Electrochemical Society, **152** 11 (2005) A2170-A2178

[30] Jun Li, Quan Min Yang, Igor Zhitomirsky, "*Nickel foam-based manganese dioxide–carbon nanotube composite electrodes for electrochemical supercapacitors*", Journal of Power Sources **185** (2008) 1569–1574

[31] Kyung-Wan Nama, Chang-Wook Lee, Xiao-Qing Yang, ByungWon Choc, Won-Sub Yoon, Kwang-Bum Kim, "*Electrodeposited manganese oxides on three-dimensional carbon nanotube substrate: Supercapacitive behavior in aqueous and organic electrolytes*", Journal of Power Sources **188** (2009) 323–331

[32] Wei-Chuan Fang, Oliver Chyan, Chia-Liang Sun, Chien-Ting Wu, Chin-Pei Chen, Kuei-Hsien Chen, Li-Chyong Chen, Jin-Hua Huang "*Arrayed CNx NT–RuO_2 nanocomposites directly grown on Ti-buffered Si substrate for supercapacitor applications*", Electrochemistry Communications **9** (2007) 239–244,

[33] Jun Yan, Zhuangjun Fan, TongWei, Jie Cheng, Bo Shao, Kai Wang, Liping Song, Milin Zhang, "*Carbon nanotube/MnO_2 composites synthesized by microwave-assisted method for supercapacitors with high power and energy densities*", Journal of Power Sources **194** (2009) 1202–1207

[34] Jae-Kyung Lee, Habib M. Pathan, Kwang-Deog Jung, Oh-Shim Joo, "*Electrochemical capacitance of nanocomposite films formed by loading carbon nanotubes with ruthenium oxide*", Journal of Power Sources **159** (2006) 1527–1531

[35] Ji-Young Kim, Kwang Heon Kim, Kwang Bum Kim, "*Fabrication and electrochemical properties of carbon nanotube / polypyrrole composite film electrodes with controlled pore size*", Journal of Power Sources **176** (2008) 396–402

[36] Zhen Fan, Jinhua Chen, Bing Zhang, Feng Sun, Bo Liu, Yafei Kuang, "*Electrochemically induced deposition method to prepare γ -MnO_2/multi-walled carbon nanotube composites as electrode material in supercapacitors*", Materials Research Bulletin **43** (2008) 2085–2091

[37] Kyung-Wan Nama, Kwang-Heon Kim, Eun-Sung Lee,Won-Sub Yoon, Xiao-Qing Yang, Kwang-Bum Kim "*Pseudocapacitive properties of electrochemically prepared nickel oxides on 3-dimensional carbon nanotube film substrates*", Journal of Power Sources **182** (2008) 642–652,

[38] Chin-Yi Chen, Tzu-Chin Chien, Yu-Chen Chan, Chung-Kwei Lin, Sheng-Chang Wang, "*Pseudocapacitive properties of carbon nanotube/manganese oxide electrode deposited by electrophoretic deposition*", Diamond & Related Materials **18** (2009) 482–485

[39] Yaohui Wang, Hao Liu, Xueliang Sun and Igor Zhitomirsky, "*Manganese dioxide–carbon nanotube nanocomposites for electrodes of electrochemical supercapacitors*", Scripta Materialia **61** (2009) 1079-1082

[40] Ji Yeong Lee, Kui Liang, Kay Hyeok An, Young Hee Lee, "*Nickel oxide/carbon nanotubes nanocomposite for electrochemical capacitance*", Synthetic Metals **150** (2005) 153–157

[41] Zhen Fan, Jinhua Chen, Mingyong Wang, Kunzai Cui, Haihui Zhou, Yafei Kuang, "*Preparation and characterization of manganese oxide/CNT composites as supercapacitive materials*", Diamond & Related Materials **15** (2006) 1478–1483